

NASA-CR-203816

FWMC  
11-92-02  
02/198

**FINAL PROGRESS REPORT**

**"DETERMINATION OF CORONAL  
MAGNETIC FIELDS FROM VECTOR  
MAGNETOGRAMS"**



**Science Applications International Corporation**

*An Employee-Owned Company*

**FINAL PROGRESS REPORT**

**“DETERMINATION OF CORONAL  
MAGNETIC FIELDS FROM VECTOR  
MAGNETOGRAMS”**



**Science Applications International Corporation**  
*An Employee-Owned Company*

Final progress report on work performed under contract  
NASW-4728  
with NASA (Solar Physics Supporting Research and Technology)

**ZORAN MIKIĆ , Principal Investigator**

10260 Campus Point Drive, San Diego, California 92121 (619) 546-6000

*Other SAIC Offices: Albuquerque, Boston, Colorado Springs, Dayton, Huntsville, Las Vegas, Los Angeles, McLean, Oak Ridge, Orlando, Palo Alto, Seattle, and Tucson*

## 1. INTRODUCTION

This report covers technical progress during the final year of the contract entitled "Determination of Coronal Magnetic Fields from Vector Magnetograms," NASW-4728, between NASA and Science Applications International Corporation, and covers the period January 1, 1994 to December 31, 1994. Under this contract SAIC has conducted research into the determination of coronal magnetic fields from vector magnetograms, including the development and application of algorithms to determine force-free coronal fields above selected observations of active regions. The contract began on June 30, 1992 and was completed on December 31, 1994. This document is the Final Report for this project.

During the present contract we developed an *evolutionary technique* for the determination of force-free (non-constant- $\alpha$ ) coronal magnetic fields from vector magnetograph observations, we demonstrated that it is possible to determine coronal magnetic fields from photospheric measurements, and we compared the estimated coronal magnetic fields of several active regions with observations. We also studied the theoretical properties of coronal arcades and helmet streamers, and demonstrated that coronal mass ejections can be initiated by photospheric shear.

The following recent publications have been sponsored by this research contract:

- McClymont, A. N., & Mikić, Z. 1994, "Thickness Variations along Coronal Loops Inferred from Vector Magnetograph Data," *Ap. J.*, **422**, 899.
- Mikić, Z., & Linker, J. A. 1994, "Disruption of Coronal Magnetic Field Arcades," *Ap. J.*, **430**, 898.
- Mikić, Z., & McClymont, A. N. 1994, "Deducing Coronal Magnetic Fields From Vector Magnetograms," in *Solar Active Region Evolution: Comparing Models with Observations* (K. S. Balasubramaniam and G. W. Simon, eds.), Astronomical Society of the Pacific Conference Series, **68**, 225.
- Linker, J. A., & Mikić, Z. 1994, "Evolution and Disruption of Magnetic Arcades," in *Solar Active Region Evolution: Comparing Models with Observations* (K. S. Balasubramaniam and G. W. Simon, eds.), Astronomical Society of the Pacific, Conference Series, **68**, 251.
- Linker, J. A., Mikić, Z., & Schnack, D. D. 1994, "Modeling Coronal Evolution," *Proc. Third SOHO Workshop - Solar Dynamic Phenomena and Solar Wind Consequences*, Estes Park, Colorado, USA, p. 249 (ESA SP-373, Dec. 1994).
- Linker, J. A., & Mikić, Z. 1995, "Disruption of a Helmet Streamer by Photospheric Shear," *Ap. J.*, **438**, L45.

## 2. SUMMARY

During the course of the present contract we developed an “evolutionary technique” for the determination of force-free coronal magnetic fields from vector magnetograph observations. The method can successfully generate nonlinear force-free fields (with non-constant- $\alpha$ ) that match vector magnetograms. We demonstrated that it is possible to determine coronal magnetic fields from photospheric measurements, and we applied it to vector magnetograms of active regions. We have also studied theoretical models of coronal fields that lead to disruptions. Specifically, we have

- demonstrated that the determination of force-free fields from exact boundary data is a well-posed mathematical problem, by verifying that the computed coronal field agrees with an analytic force-free field (Low & Lou 1990) when boundary data for the analytic field are used;
- demonstrated that it is possible to determine active-region coronal magnetic fields from photospheric measurements, by computing the coronal field above active region 5747 on 20 October 1989 (Mikić & McClymont 1994), AR6919 on 15 November 1991 (Mikić & McClymont 1994), and AR7260 on 18 August 1992 (McClymont & Mikić 1993), from data taken with the Stokes Polarimeter at Mees Solar Observatory, University of Hawaii;
- started to analyze active region 7201 on 19 June 1992 using measurements made with the Advanced Stokes Polarimeter at NSO/Sac Peak (Martínez Pillet *et al.* 1994; Lites *et al.* 1995);
- investigated the effects of imperfections in the photospheric data on the computed coronal magnetic field;
- documented the coronal field structure of AR5747 and compared it to the morphology of footpoint emission in a flare, showing that the “high-pressure” H- $\alpha$  footpoints are connected by coronal field lines (Mikić & McClymont 1994);
- shown that the variation of magnetic field strength along current-carrying field lines is significantly different from the variation in a potential field, and that the resulting near-constant area of elementary flux tubes is consistent with observations (McClymont & Mikić 1994);
- begun to develop realistic models of coronal fields which can be used to study flare trigger mechanisms (Mikić 1993);
- demonstrated that magnetic nonequilibrium can disrupt sheared coronal arcades (Mikić & Linker 1994), and that helmet streamers can disrupt, leading to coronal mass ejections (Linker & Mikić 1995).

Our model has significantly extended the realism with which the coronal magnetic field can be inferred from actual observations. In a subsequent contract awarded by NASA (SR&T Contract NASW-5017, “Determination and Modeling of Active-Region Magnetic Fields”), we have continued to apply and improve the

evolutionary technique, to study the physical properties of active regions, and to develop theoretical models of magnetic fields.

### 3. TECHNICAL PROGRESS

During the current contract period we demonstrated the merits of the principle of computing force-free fields from observational data. The results are very encouraging: it is indeed possible to obtain a good estimate of the coronal magnetic field from vector magnetograms. Our model has significantly extended the realism with which the coronal magnetic field can be inferred from observations. In addition to demonstrating the viability of the method, two results of physical interest have been obtained: we have shown that two high-pressure H- $\alpha$  footpoints observed during a flare are connected, lying at opposite ends of coronal field lines, and that the area variation along current-carrying flux tubes is consistent with the observed constant width of many soft X-ray loops (Section 3.3). On the modeling front, we have demonstrated that photospheric shear can disrupt coronal arcades and helmet streamers (Section 3.4), which may explain the mechanism that initiates coronal mass ejections.

#### 3.1 An "Evolutionary Technique" for Determination of Coronal Fields

Ever since the development of magnetographs there has been considerable interest in deducing coronal magnetic fields from observations. In the simplest approximation it has been assumed that the coronal field is given by a potential field, *i.e.*, that the corona is current-free (Schmidt 1964; Teuber, Tandberg-Hanssen, & Hagyard 1977; Gary *et al.* 1987). However, since potential fields are minimum-energy states, this model is generally not adequate for describing the highly sheared fields observed in active regions.

The force-free approximation  $\mathbf{J} \times \mathbf{B} = 0$  provides a good description of the quasi-static evolution of the strong coronal magnetic field above an active region (Sturrock & Woodbury 1967). Therefore, the electric current is everywhere parallel to the magnetic field,  $\mathbf{J} = \alpha \mathbf{B}$ , which implies that the magnetic field satisfies the nonlinear equation

$$\frac{c}{4\pi} \nabla \times \mathbf{B} = \alpha \mathbf{B} . \quad (1)$$

The torsion  $\alpha = \alpha(\mathbf{x})$ , which obeys the equation  $\mathbf{B} \cdot \nabla \alpha = 0$ , is to be determined as part of the solution. Equation (1) needs to be solved with the appropriate boundary conditions at the photosphere and at infinity. In this application, the boundary conditions at the photosphere are required to appropriately match data measured with a vector magnetograph (see below).

This boundary-value problem has a solution when appropriate boundary conditions are specified (Schmidt 1968; Bineau 1972; Aly 1984, 1988, 1989). A well-posed formulation requires the specification of the normal magnetic field  $B_n$  and the normal component of the current density  $J_n$  (in the region with  $B_n > 0$ ) on the boundary. Since a vector magnetogram measures all three components of the magnetic field in the observation plane (after the 180° ambiguity in the transverse

field is resolved), the vertical field  $B_n$  can be determined in a straightforward manner;  $J_n$  is deduced from horizontal derivatives of the horizontal field. It is important to note that the determination of the force-free coronal field is mathematically well-posed when formulated in this way. Indeed, Molodensky (1974) has shown that the force-free field is stable with respect to changes in the boundary data to the same extent that the potential field is.

Considerable simplification results if it is assumed that  $\alpha$  is a constant, reducing the problem to a linear one (Nakagawa & Raadu 1972; Chiu & Hilton 1977; Alissandrakis 1981; Hannakam, Gary, & Teuber 1984). Levine (1975, 1976) has reviewed the application of such models to observations, and has concluded that the constant- $\alpha$  model is inadequate for describing coronal fields.

The nonlinear problem with non-constant- $\alpha$  has also been tackled: Sakurai (1981) devised an iterative solution which relies on field line tracing; however, the scheme does not always converge, especially in situations with high shear and complicated topology, which are present in active regions. Wu *et al.* (1990) have proposed an "extrapolation scheme" that is exponentially sensitive to measurement errors at the boundary, and can only give estimates of the field at low coronal heights and inevitably breaks down at higher coronal altitudes (Gary & Musielak 1992).

The basis of our coronal force-free field solution relies on a new formulation of this boundary-value problem. In our algorithm, the force-free solution is found using an *evolutionary* approach. Instead of directly solving the equilibrium equation (1), we solve a related time-dependent problem whose steady-state solution satisfies the force-free equation and the boundary data. The method finds solutions to the boundary-value problem by dynamically adjusting the electric current in the corona to match the observed boundary data. The field is relaxed toward a steady state with boundary conditions applied to the magnetic flux and transverse electric field. An adaptive external circuit drives the plasma to a state in which the normal electric current density  $J_n$  at the photosphere matches the observed current density. The use of a finite plasma resistivity allows the field to change topology during its relaxation to a steady state. Roumeliotis (1994) describes a similar scheme with an alternative implementation of photospheric boundary conditions.

### 3.2 Application of the Evolutionary Technique

For active-region length scales ( $\sim 100,000$  km) it is possible to neglect the curvature of the solar surface. The active region is enclosed in the rectangular domain  $\{0 \leq x \leq L_x; 0 \leq y \leq L_y; 0 \leq z \leq L_z\}$ , where  $z$  represents height in the corona, and  $z = 0$  represents the photosphere. The box dimensions are made large compared to the dimensions of the active region, to isolate the active region from the artificial numerical boundaries (at  $x = 0$  and  $L_x$ ;  $y = 0$  and  $L_y$ ; and  $z = L_z$ ), which are assumed to be perfectly conducting walls at which we set  $B_n = 0$  and  $\mathbf{v} = 0$ , where  $\mathbf{v}$  is the plasma flow velocity. The 3D time-dependent MHD equations are solved using finite differences in space and time (*e.g.*, Mikić, Barnes, & Schnack 1988; Mikić, Schnack, & Van Hoven 1989, 1990; Mikić & Linker 1994). Nonuniform meshes are used to maximize the resolution within the active region, while at the same time

surrounding it in a large computational domain to minimize the effect of lateral boundaries.

The vector magnetograms are reduced at the University of Hawaii. The line-of-sight field and the magnitude and azimuth of the transverse field are deduced from the measured Stokes profiles using the method of Skumanich and Lites (1987), combined with an integral method in weak-field regions (Ronan, Mickey, & Orrall 1987). The  $180^\circ$  ambiguity in the transverse field direction is resolved, and the magnetic fields are transformed to a local Cartesian coordinate system in heliospheric coordinates to give  $B_x$ ,  $B_y$ , and  $B_z$  in the photospheric plane  $z = 0$ . The normal component of the current density at  $z = 0$ , which is required as a boundary condition in the evolutionary technique, is determined by differentiation of the horizontal fields,  $J_z = (4\pi/c)(\partial B_y/\partial x - \partial B_x/\partial y)$ . The details of the reduction are given by Canfield *et al.* (1993).

The calculation begins at  $t = 0$  with a potential field corresponding to the measured flux  $B_z$  at the photospheric boundary at  $z = 0$ . The potential magnetic field is determined from  $\mathbf{B} = \nabla\phi$ , where  $\phi$  is the solution to the 3D potential field equation  $\nabla^2\phi = 0$ , with  $\partial\phi/\partial z = B_z$  at  $z = 0$ . Subsequently, the coronal field evolves in response to an adaptive boundary circuit in which the transverse electric field at  $z = 0$  is varied in such a manner as to force the current density  $J_z$  to match the distribution deduced from the magnetogram. In steady state the coronal field approaches a force-free state that satisfies the required boundary conditions on  $B_z$  and  $J_z$ .

We have verified that this technique can correctly estimate the coronal field when the boundary data corresponding to an analytic force-free field is used. The boundary data from the nonlinear analytic force-free field of Low and Lou (1990) was used to specify  $B_z$  and  $J_z$  at  $z = 0$  in the evolutionary technique, which was then used to estimate the coronal field. Figure 1 shows a comparison between the field lines in the analytic solution and those in the coronal field determined from the boundary data. This simulates the application of the evolutionary technique to a vector magnetogram, albeit to one with perfectly consistent data. The excellent agreement between the estimated coronal magnetic field and the analytic solution verifies that the evolutionary technique is based on a well-posed formulation.

Aly (1984, 1988, 1989) has noted that a force-free field satisfies several integral constraints that can be checked using only values of the measured photospheric magnetic field. We have used these constraints to screen candidate vector magnetograms for suitability. Violation of these constraints will degrade the accuracy of estimated coronal fields. In addition, the magnetic field may not be force-free where it is measured at the photosphere, although this is not expected to be a severe limitation (Aly 1989). Our initial experience with the evolutionary technique indicates that it does not appear to be overly sensitive to such discrepancies, although this matter is still under investigation.

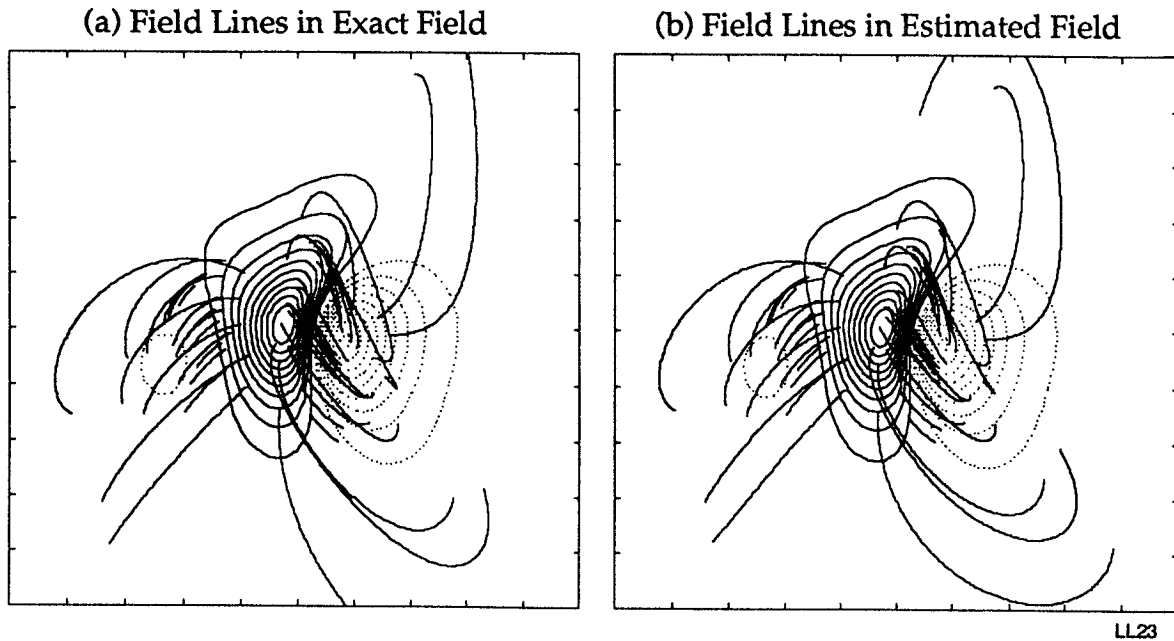


Figure 1.—Comparison between field lines in (a) the analytic force free field of Low & Lou (1990), and (b) the coronal field estimated using the evolutionary technique from the boundary data at  $z = 0$ . The contours show the vertical magnetic field. The excellent agreement shows that the evolutionary technique is based on a well-posed mathematical formulation.

### 3.3 Properties of Coronal Magnetic Fields: Comparison with Observations

NOAA active region 5747 was observed at Mees Solar Observatory (MSO) during its transit across the solar disk during October 1989; coordinated observations were also made at Big Bear Solar Observatory. Daily vector magnetograms were taken at MSO for each of the five days during the period 18 October through 22 October 1989, using the Haleakala Stokes Polarimeter. This active region showed highly nonpotential photospheric vector magnetic field structure and produced many solar flares, three of which were observed at MSO (Leka *et al.* 1993). The data for the third of the five days (20 October) proved to be the most suitable for analysis, mainly because most of the flux of the active region was captured in the magnetogram. When applied to this magnetogram, the evolutionary technique converges to a steady-state solution in several hundred Alfvén times. Figure 2 shows traces of magnetic field lines in the estimated coronal field, as well as the field lines in the potential magnetic field for comparison. The estimated field has significant twist compared to the potential field. These field line traces show reasonable agreement with features that can be identified in an  $H\text{-}\alpha$  image taken at Big Bear Solar Observatory. The potential field has a magnetic energy equal to  $1.44 \times 10^{33}$  ergs, while the estimated coronal field has an energy of  $1.89 \times 10^{33}$  ergs, indicating that the coronal field is significantly nonpotential.



AR5747, 20 October 1989

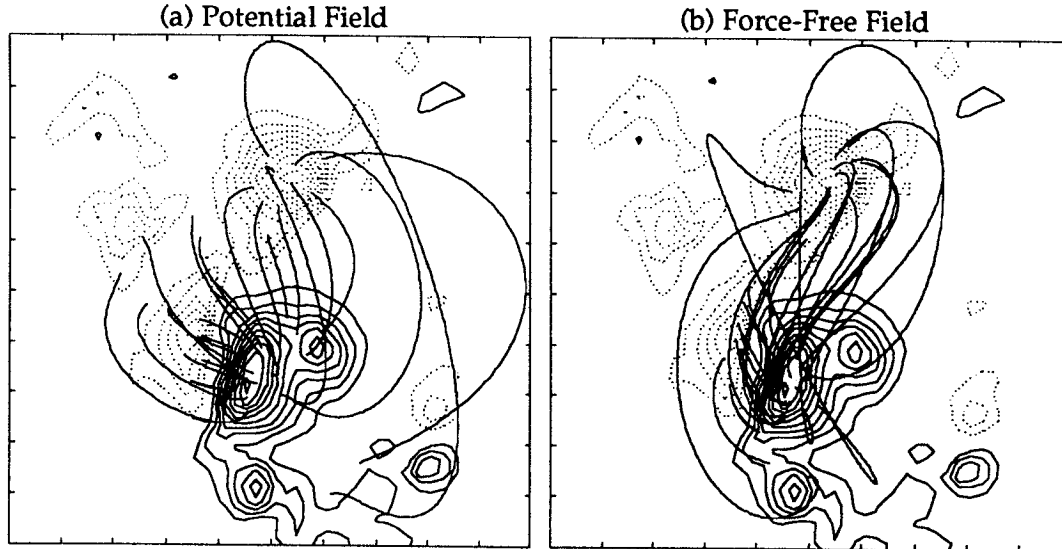


Figure 2.—Traces of the field lines in (a) the potential coronal field of active region 5747 on October 20, 1989, and (b) the estimated force-free field as determined from a vector magnetogram. The contours show the vertical magnetic field  $B_z$  in the photosphere. The figure covers an area of  $100,000 \times 100,000$  km.

We have also applied this technique to two additional active regions: AR6919 on 15 November 1991 (Mikić & McClymont 1994), and AR7260 on 18 August 1992 (McClymont & Mikić 1993). Vector magnetograms of these regions were taken with the Stokes Polarimeter at Mees Solar Observatory. We have also started to analyze a  $\delta$ -spot group in active region 7201 on 19 June 1992 from measurements made with the Advanced Stokes Polarimeter at NSO/Sac Peak (Martínez Pillet *et al.* 1994; Lites *et al.* 1995).

To illustrate how the estimated coronal magnetic field might be used in studies of flare and active-region physics, we compare the connectivity implied by the coronal field with H- $\alpha$  data obtained at MSO during an M2 flare (Leka *et al.* 1993) which occurred 3 hours after the magnetogram scan was completed. Figure 3 shows observed H- $\alpha$  flare features superimposed on the magnetogram of AR5747. The three small pseudo-circular features in Fig. 3(a) enclose areas in which specific H- $\alpha$  signatures were detected. The small feature on the neutral line marked "C" showed the signature of particle precipitation and coincided temporally with hard X-ray emission. Figs. 3(b) and (c) (refer to the caption) show that the footpoints of a coronal loop in the estimated force-free coronal field are in much closer agreement with the observed high-pressure regions than footpoints of a loop in the potential magnetic field. It is unfortunate that there are no soft X-ray observations of AR5747 to confirm the existence of a high-pressure coronal loop joining the H- $\alpha$  footpoints.

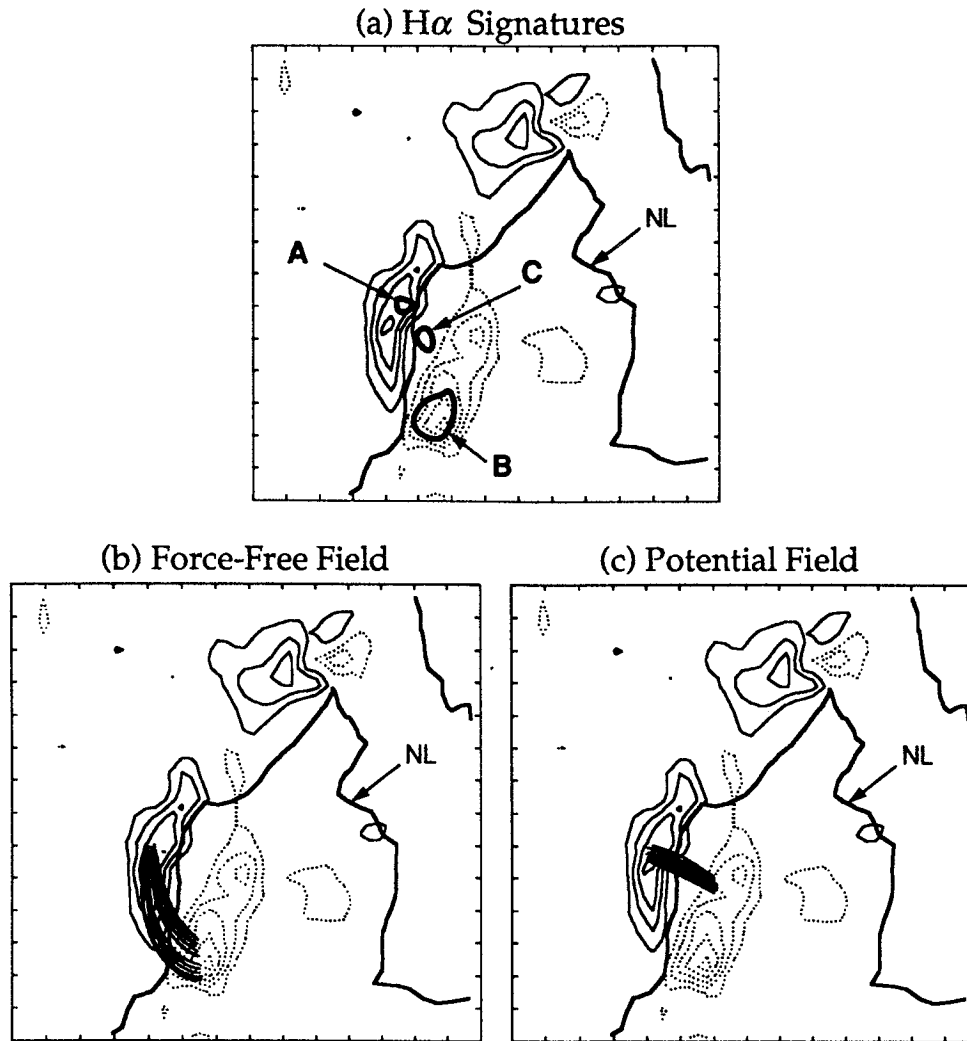


Figure 3.—(a)  $H\alpha$  flare features superimposed on the magnetogram of AR5747 (adapted from Leka *et al.* 1993). The dark line marked “NL” denotes the magnetic neutral line; the contours denote the vertical current density (solid  $J_z > 0$ , dotted  $J_z < 0$ ). The three small pseudo-circular features enclose areas in which specific  $H\alpha$  signatures were detected. The features marked “A” and “B” show sites which were identified as high pressure “footpoints,” whereas “C” was identified as an electron precipitation site. (b) Field line traces in the estimated force-free coronal field, showing that the high-pressure sites A and B are close to the footpoints of a coronal loop. (c) Field line traces in the potential coronal field, with the same initial footpoint positions (at A) as in (b), showing that the agreement between the high-pressure sites and coronal loop footpoints is much better for the estimated force-free field than for a potential field.

Since the Skylab era it has been noted that images of coronal loops seen in soft X-rays or extreme ultraviolet emission appear to be of remarkably uniform thickness, a result recently confirmed by high-resolution observations (Golub 1991; Klimchuk, Canfield, & Rhoads 1992). If the emitting volume outlines a bundle of field lines, or flux tube, the implication is that the magnetic field does not expand in height as it would if the field were potential. Recently Klimchuk *et al.* (1992) have quantified this characteristic, finding for several loops observed by the Soft X-ray Telescope on the Yohkoh spacecraft a thickness variation along their lengths of only 10–20%. We have demonstrated that this observation is consistent with the characteristics of current-carrying field lines in a highly sheared active region. By tracing field lines in the computed coronal field for AR5747 we have shown that magnetic loops which are highly sheared do not expand rapidly in height, as they would in a potential field (McClymont & Mikić 1994).

### 3.4 Disruption of Arcades and Helmet Streamers

The evolution of coronal arcades in response to applied shearing photospheric flows indicates that disruptive behavior can occur beyond a critical shear. The ideal and resistive properties of isolated large-scale coronal magnetic arcades were studied using axisymmetric solutions of the time-dependent MHD equations in spherical geometry. The disruption can be traced to ideal MHD magnetic nonequilibrium. The magnetic field expands outward in a process that opens the field lines and produces a tangential discontinuity in the magnetic field. In the presence of plasma resistivity, the resulting current sheet is the site of rapid reconnection, leading to an impulsive release of magnetic energy, fast flows, and the ejection of a plasmoid (Mikić & Linker 1994). When a more realistic model with a solar wind is used, we find that photospheric shear can cause helmet streamers to disrupt, leading to coronal mass ejections (Linker & Mikić 1995).

## 5. REFERENCES

- Alissandrakis, C. E. 1981, *Astron. Astrophys.*, **100**, 197
- Aly, J. J. 1984, *Ap. J.*, **283**, 349
- Aly, J. J. 1988, *Astron. Astrophys.*, **203**, 183
- Aly, J. J. 1989, *Solar Phys.*, **120**, 19
- Bineau, M. 1972, *Comm. Pure Appl. Math.*, **25**, 77
- Canfield, R. C., de La Beaujardière, J.-F., Fan, Y., Leka, K. D., McClymont, A. N., Metcalf, T. R., Mickey, D. L., Wülser, J.-P., & Lites, B. W. 1993, *Ap. J.*, **411**, 362
- Chiu, Y. T., & Hilton, H. H. 1977, *Ap. J.*, **212**, 873
- Gary, G. A., Moore, R. L., Haggard, M. J., & Haisch, B. M. 1987, *Ap. J.*, **314**, 782
- Gary, G. A., & Musielak, Z. E. 1992, *Ap. J.*, **392**, 722
- Golub, L. 1991, in *Mechanisms of Chromospheric and Coronal Heating*, P. Ulmschneider, E. R. Priest, & R. Rosner (eds.), (Berlin: Springer-Verlag), p. 115
- Hannakam, L., Gary, G. A., & Teuber, D. L. 1984, *Solar Phys.*, **94**, 219
- Klimchuk, J. A., Canfield, R. C., & Rhoads, J. E. 1992, *Ap. J.*, **385**, 327
- Leka, K. D., Canfield, R. C., McClymont, A. N., de La Beaujardière, J.-F., Fan, Y., & Tang, F. 1993, *Ap. J.*, **411**, 370
- Levine, R. H. 1975, *Solar Phys.*, **44**, 365
- Levine, R. H. 1976, *Solar Phys.*, **46**, 159
- Linker, J. A., & Mikić, Z. 1995, *Ap. J.*, **438**, L45
- Lites, B. W., Low, B. C., Martínez Pillet, V., Seagraves, P., Skumanich, A., Frank, Z. A., Shine, R. A., and Tsuneta, S. 1995, *Ap. J.*, **446**, 877
- Low, B. C., and Lou, Y. Q. 1990, *Ap. J.*, **352**, 343
- Martínez Pillet, V., Lites, B. W., Skumanich, A., & Degenhardt, D. 1994, *Ap. J.*, **425**, L113
- McClymont, A. N., & Mikić, Z. 1993, presented at the Yokohama Coordinated Data Analysis Workshop, held in Hawaii, December 1993
- McClymont, A. N., & Mikić, Z. 1994, *Ap. J.*, **422**, 899
- Mikić, Z., Barnes, D. C., & Schnack, D. D. 1988, *Ap. J.*, **328**, 830
- Mikić, Z., Schnack, D. D., & Van Hoven, G. 1989, *Ap. J.*, **338**, 1148
- Mikić, Z., Schnack, D. D., & Van Hoven, G. 1990, *Ap. J.*, **361**, 690
- Mikić, Z. 1993, Solar Physics Division Meeting, Palo Alto, CA, July 13–16
- Mikić, Z., & Linker, J. A. 1994, *Ap. J.*, **430**, 898
- Mikić, Z., & McClymont, A. N. 1994, "Deducing Coronal Magnetic Fields From Vector Magnetograms," in *Solar Active Region Evolution: Comparing Models with Observations* (K. S. Balasubramaniam and G. W. Simon, eds.), Astronomical Society of the Pacific Conference Series, **68**, 225
- Molodensky, M. M. 1974, *Solar Phys.*, **39**, 393
- Nakagawa, Y., & Raadu, M. A. 1972, *Solar Phys.*, **25**, 127
- Ronan, R. S., Mickey, D. L., & Orrall, F. Q. 1987, *Solar Physics*, **113**, 353
- Roumeliotis, G. 1994, preprint
- Sakurai, T. 1981, *Solar Physics*, **69**, 343
- Schmidt, H. U. 1964, in *AAS–NASA Symposium on the Physics of Solar Flares*, NASA SP-50, p. 107

- Schmidt, H. U. 1968, in *Structure and Development of Solar Active Regions*, IAU Symposium No. 35, ed. K. O. Kiepenheuer (Dordrecht: Reidel), p. 95
- Skumanich, A., & Lites, B. W. 1987, *Ap. J.*, **233**, 473
- Sturrock, P.A., and Woodbury, E.T. 1967, in *Plasma Astrophysics, Proc. of the International School of Physics "Enrico Fermi," Course 39*, ed. P. A. Sturrock (New York: Academic Press), p. 155
- Teuber, D., Tandberg-Hanssen, E., & Hagyard, M. J. 1977, *Solar Phys.*, **53**, 97
- Wu, S. T., Sun, M. T., Chang, H. M., Hagyard, M. J., & Gary, G. A. 1990, *Ap. J.*, **362**, 698